Cell Reports, Volume *43*

Supplemental information

Selective targeting of mu opioid receptors to primary cilia

Rita R. Fagan, David F. Lee, Matan Geron, Grégory Scherrer, Mark von Zastrow, and Aliza T. Ehrlich

Table S1: Primers used for DNA construct molecular cloning.

Construct	Forward Primer 1	Reverse Primer 1	Forward Primer 2	Reverse Primer 2
MOR	ACGCCGCTGGAGCA GCGGCCATGGATAG CTCTGCCGGCCCTG	TCTAGAGTCGCGGCCTCAAGG CAGGGGGGCTG	N/A	N/A
MOR+linker	ACGCCGCTGGAGCA GCGGCCATGGATAG CTCTGCCGGCCCTG	TCTAGAGTCGCGGCCTCAGGT AGCAATAGAGCCAGGC	N/A	N/A
MOR-Venus	ACGCCGCTGGAGCA GCGGCCATGGATAG CTCTGCCGGCCCTG	TCTAGAGTCGCGGCCTTACTTA TACAGCTCGTCCATGCC	N/A	N/A
MOR+5A	ACGCCGCTGGAGCA GCGGCCATGGATAG CTCTGCCGGCCCTG	TCTAGAGTCGCGGCCTCAAGC AGCAGCAGCAGCAGGCAGGG	N/A	N/A
DOR	GCTGGAGCAGCGGC CATGGAGCTGGTGC CCT	TCTAGAGTCGCGGCCTCAGGC GGCAGCGC	N/A	N/A
DOR+linker	GCTGGAGCAGCGGC CATGGAGCTGGTGC CCT	GCGGCCTCAGGTAGCAATAGA GCCGGCGGCAGC	N/A	N/A
KOR	GCTGGAGCAGCGGC CATGGAGTCCCCCAT TCAGATCTTC	TCTAGAGTCGCGGCCTCATAC TGGCTTATTCATCCCTCCCAC	N/A	N/A
KOR+linker	GCTGGAGCAGCGGC CATGGAGTCCCCCAT TCAGATCTTC	GCGGCCTCAGGTAGCAATAGA GCCTACTGGCTT	N/A	N/A
MOR(DOR-ICL3)+linker	ACGCCGCTGGAGCA GCGGCCATGGATAG CTCTGCCGGCCCTG	TGATCTAGAGTCGCGGCCTCA GGTAGCAATAGAGCCAGGC	N/A	N/A
MOR(DOR-Ctail)+linker	ACGCCGCTGGAGCA GCGGCCATGGATAG CTCTGCCGGCCCTG	GCGGCCTCAGGTAGCAATAGA GCCGGCGGCAGC	N/A	N/A
DOR(MOR-ICL3)+linker	GCTGGAGCAGCGGC CATGGAGCTGGTGC CCT	GCGGCCTCAGGTAGCAATAGA GCCGGCGGCAGC	N/A	N/A
DOR(MOR-Ctail)+linker	GCTGGAGCAGCGGC CATGGAGCTGGTGC CCT	TCTAGAGTCGCGGCCTCAGGT AGCAATAGAGCCAGGC	N/A	N/A
MOR(381T)+linker	ACGCCGCTGGAGCA GCGGCCATGGATAG CTCTGCCGGCCCTG	AGTCGCGGCCTCAGGTAGCAA TAGAGCCGTCCACGGTGT	N/A	N/A
DOR+MOR3+linker	GCTGGAGCAGCGGC CATGGAGCTGGTGC CCT	TCTAGAGTCGCGGCCTCAGGT AGCAATAGAGCCAGGCAGGG GGGCGGCAGCGCCACC	N/A	N/A
DOR+MOR5+linker	GCTGGAGCAGCGGC CATGGAGCTGGTGC CCT	AGAGTCGCGGCCTCAGGTAG CAATAGAGCCAGGCAGGGGG GCTGTGGCGGCAGCGCC	N/A	N/A
DOR+MOR12+linker	GCTGGAGCAGCGGC CATGGAGCTGGTGC CCT	TTCCAGGTTTTCCAGGGCGGC AGCGCCACC	GGTGGCGCTGCCGC CCTGGAAAACCTGG AA	TCTAGAGTCGCGGCCTCAGG TAGCAATAGAGCCAGGC
DOR+MOR17+linker	GCTGGAGCAGCGGC CATGGAGCTGGTGC CCT	CTGGTGGTTGGTCCTGGCGG CAGCGCCACC	GGTGGCGCTGCCGC CAGGACCAACCACC AG	TCTAGAGTCGCGGCCTCAGG TAGCAATAGAGCCAGGC
TULP3-eGFP	GAAGATCTTGCGGC CGAGGCGGCGCGC	TCTAGAGTCGCGGCCGCTCAT TCACACGCCAGCTTG	TTTTGGCAAAGAATT CATGGAGGCGGCGC	CACCATGGTGGAATTACTACC TGATCCACTACCTTCACACGC CA
TULP3(201T)-eGFP	GAAGATCTTGCGGC CGAGGCGGCGCGC	TCTAGAGTCGCGGCCTCATCC AAGCTGGGCGTCAC	TTTTGGCAAAGAATT CATGGAGGCGGCGC	CACCATGGTGGAATTACTACC TGATCCACTACCTCCAAGCTG

Table S2: Experiment time-line and corresponding figures for endogenous MOR staining in primary habenula culture (related to **Figure 1** and **Figure S1**).

Experiment Day	Antigen	Primary	Secondary	False Positives	Figure
Day 1	MOR	Rb anti-MOR			
Day 2 (am)			Anti-rb-488	None	
Day 2 (pm)	AC3	Rb anti-AC3			
Day 3			Anti-rb-647	647 may detect MOR and AC3	**Figure 1F,** **Control: Figure S1D**
or					
Day 2 (pm)	ARL13B	Rb anti-ARL13B			
Day 3			Anti-rb-647	647 may detect MOR and ARL13B	**Figure 1F,** **Control: Figure S1E**
or					
Day 2 (pm)	ARL13B	Rb anti-ARL13B-647	None	None	**Figure S1F,** **Control: Figure S1G**
or					
Day 1	MOR + AC3	Rb anti-MOR + Chk anti-AC3			
	MOR + ARL13B	Rb anti-MOR + Ms anti-ARL13B			
Day 2	MOR + AC3		Anti-rb-488 + Anti-chk-647	None	**Figure S1H, top**
	MOR + ARL13B		Anti-rb-488 + Anti-ms-647	None	**Figure S1H, bottom**

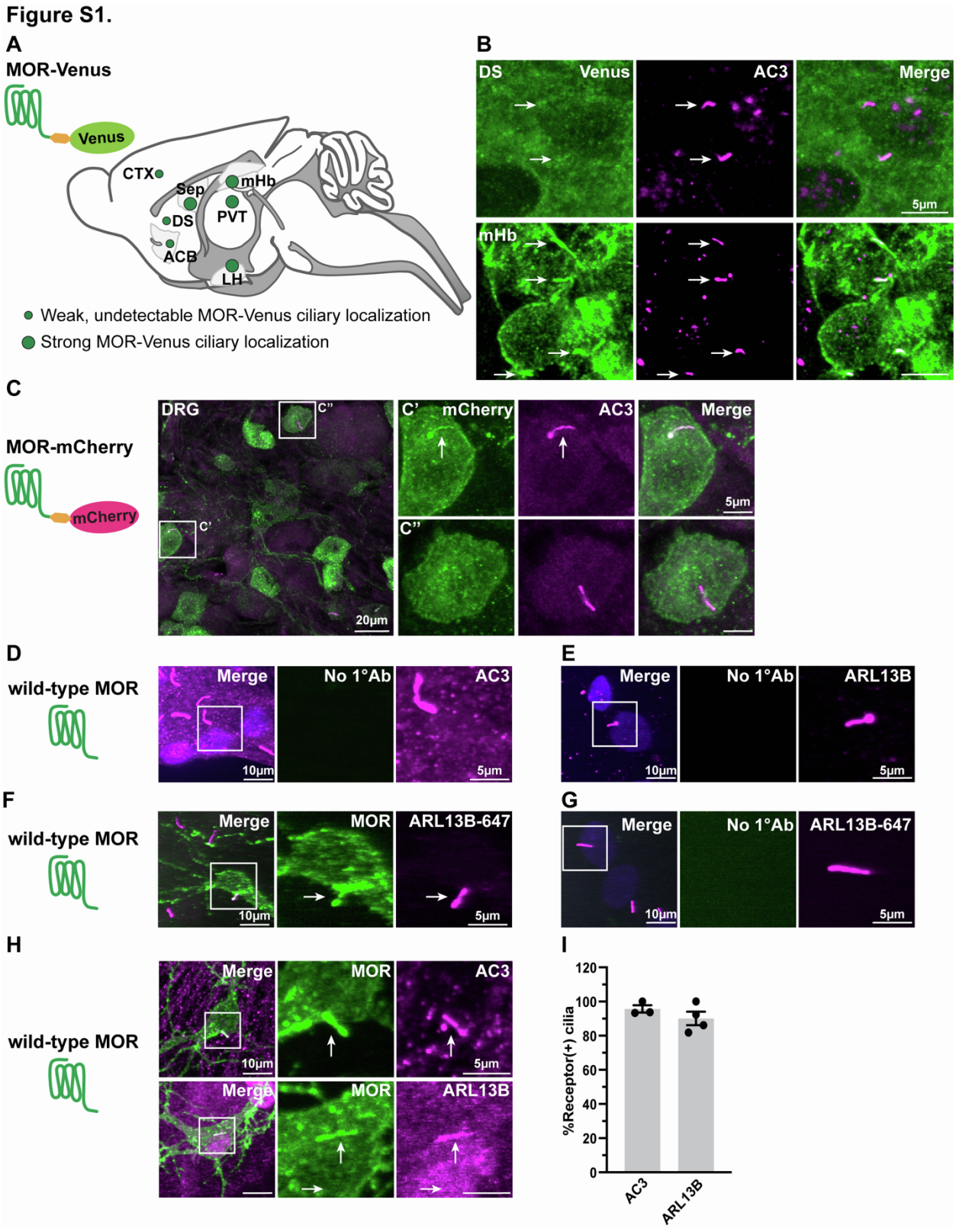

Figure S1. MOR-Venus cilia localization across multiple brain regions, MOR-mCherry localization to DRG primary cilia and wild-type MOR ciliary localization

quantification. MOR-Venus was amplified using a GFP antibody. (**A**) Schematic summary of brain regions with MOR-Venus localized to primary cilia: cortex (CTX), septum (Sep), dorsal striatum (DS), nucleus accumbens (ACB), medial habenula (mHb), paraventricular nucleus of the thalamus (PVT), and lateral hypothalamus (LH). Weak, undetectable cilia localization (small circles); strong, frequent ciliary localization (large circles). (**B**) Representative confocal micrographs depicting ciliary localized MOR-Venus in the DS (top panels) and mHb (bottom panels). Scale bars: 5μm. (**C**) Representative confocal micrograph of dorsal root ganglion (DRG) sections from 4-week old MOR-mCherry animals. mCherry signal was amplified using an mCherry antibody and cilia were identified using AC3 antibody. Scale bar: 20μm. (**C'**) Example of an mCherry-positive cell with receptor localized to primary cilium, (**C''**) is an example of an mCherry-positive cell that does not have receptor localized in the primary cilium. Scale bars: 5μm. (**D-G**) Control stainings for main text **Figure 1**. (**D-E**) Representative confocal images of E18 cultured rat habenula neurons stained with the following sequence: no 1° antibody for native MOR, anti-rabbit Alexa Fluor 488, rabbit anti-AC3 (**D**) or rabbit anti-ARL13B (**E**), and anti-rabbit Alexa Fluor 647 to control for aberrant detection of ciliary MOR in AC3(+) (**D**) and ARL13B(+) (**E**) cilia. (**F**) Representative confocal micrographs of endogenous MOR localized to ARL13B-647 labeled cilia in E18 cultured rat habenula neurons. Arrows indicate wild-type MOR(+) primary cilia. (**G**) Representative confocal images of E18 cultured rat habenula neurons stained with the following sequence: no 1° antibody for MOR, anti-rabbit Alexa Fluor 488, and rabbit anti-ARL13B-647 conjugated antibody to control for aberrant detection of ciliary MOR in ARL13B(+) cilia. (**H**) Representative confocal images of E18 cultured rat habenula neurons stained with antibodies against MOR and AC3 (top) or MOR and ARL13B (bottom). Arrows indicate wild-type MOR(+) primary cilia. Scale bars (**D-H**): 10μm (merge), 5μm (individual channels). (**I**) The percent of MOR-positive cells with MOR localized to cilia was quantified using both cilia markers. The percent of MOR(+) cilia was 95.7% using AC3 and 90.1% using ARL13B; data are represented as mean ± SEM from 3 independent experiments, 75-103 neurons. Arrows indicate cilia-localized receptor.

Figure S2.

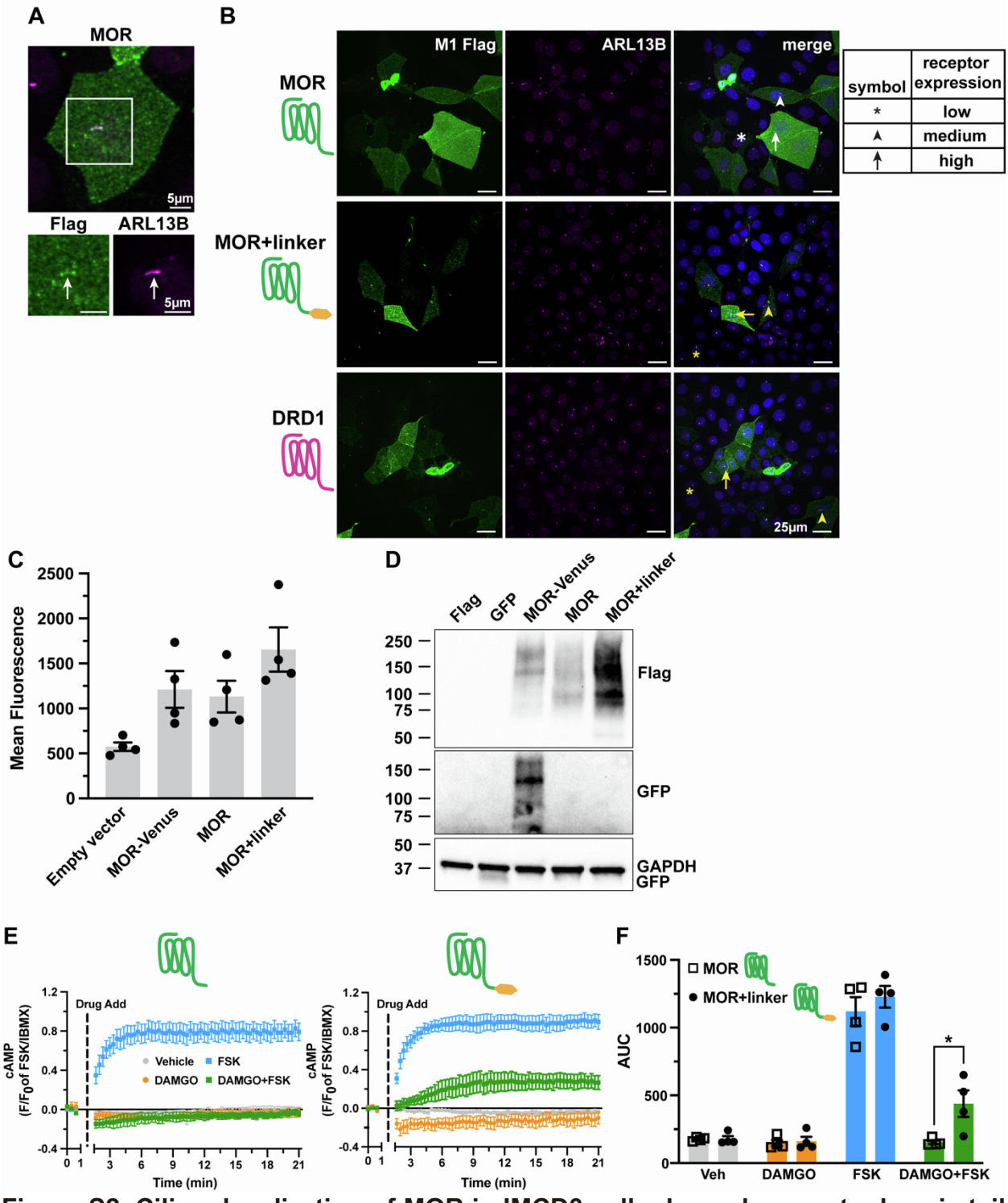

Figure S2. Ciliary localization of MOR in IMCD3 cells depends on cytoplasmic tail modification of MOR, is not a consequence of surface expression and modifies the duration of MOR cAMP signaling. (**A**) Representative confocal images of MOR(+) primary cilium. IMCD3 cells transiently expressing Flag-tagged MOR. Cilia were stained with anti-ARL13B antibody. Scale bars: 5µm. (**B-D**) Expression control for constructs

analyzed in main text **Figure 2**. (**B**) Schematics and representative micrographs of MOR, MOR+linker, and dopamine receptor type 1 (DRD1) transiently expressed in IMCD3 cells. Surface receptors were labeled with Flag M1 and cilia were stained with anti-ARL13B antibody. Asterisks indicate low receptor-expressing cells, arrow heads point out cells with medium receptor expression, and arrows indicate high receptor expression. Examples of receptor(-) cilia are indicated by white symbols and receptor(+) cilia are shown by yellow symbols. Scale bars: 25μm. (**C**) Flow cytometry analysis of IMCD3 cells transfected with empty vector, MOR-Venus, MOR, or MOR+linker indicate no significant difference between MOR and C-terminally tagged constructs. One-way ANOVA (*p=0.0107) with Dunnett's multiple comparisons, data are represented as mean ± SEM from 4 independent experiments. (**D**) Western blot depicting receptor expression levels of MOR-Venus, MOR, and MOR+linker expressed in IMCD3 cells. Equal protein was loaded into wells and blots were probed for Flag, GFP, and loading control GAPDH. (**E**) cAMP as measured by cADDis biosensor in IMCD3 cells transiently expressing MOR (left) or MOR+linker (right). Live cells were imaged for baseline fluorescence for one minute prior to drug treatment with either vehicle (grey), 1μM forskolin (FSK, blue), 1μM DAMGO (orange), or both DAMGO+FSK (green). Data are represented as mean ± SEM from from independent experiments. (**F**) Summary data of the cAMP area under the curve (AUC, positive peaks). Two-way ANOVA interaction (ns) p=0.0995; main effect of receptor (*) p=0.0259; main effect of drug (****) p<0.0001. Sidak's multiple comparisons test, data are represented as mean ± SEM from 4 independent experiments, 9-44 cells in each biological replicate, (*) p=0.0114. Arrows indicate cilia-localized receptor.

Figure S3.

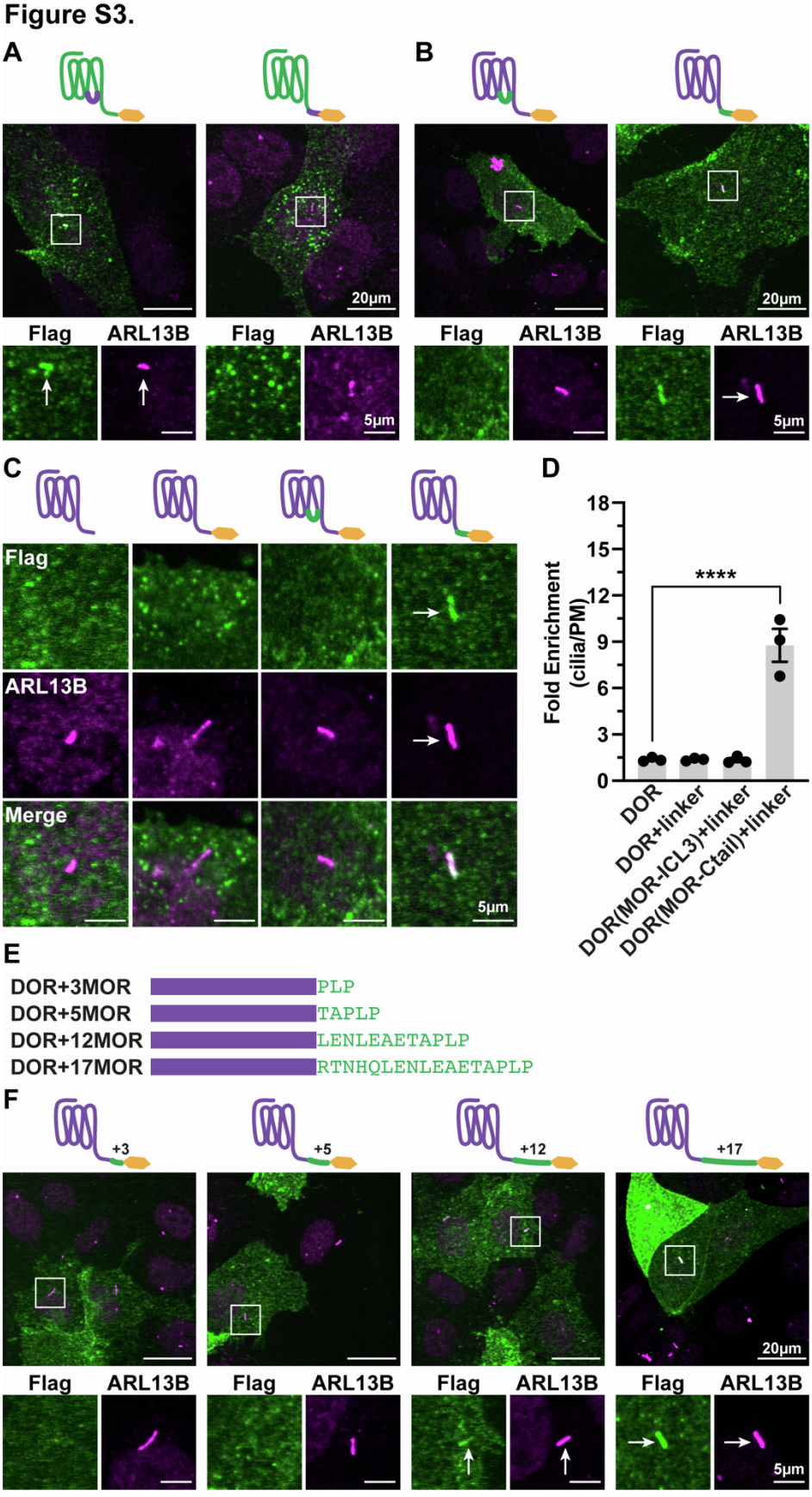
A
B
20μm
Flag
ARL13B
5μm
C
Flag
ARL13B
Merge
5μm
D
Fold Enrichment (cilia/PM)
18
15
12
9
6
3
0
****
DOR
DOR+linker
DOR(MOR-ICL3)+linker
DOR(MOR-Ctail)+linker
E
DOR+3MOR PLP
DOR+5MOR TAPLP
DOR+12MOR LENLEAETAPLP
DOR+17MOR RTNHQLENLEAETAPLP
F
+3
+5
+12
+17
20μm
Flag
ARL13B
5μm

Figure S3. The MOR C-tail is highly divergent from DOR C-tail and suffices to drive DOR cilia enrichment. (**A-B**) Plasma membrane expression validation for constructs analyzed in main text **Figure 3**. (**A**) Wide view of IMCD3 cells transiently expressing MOR(DOR-ICL3)+linker or MOR(DOR-Ctail)+linker demonstrating plasma membrane expression of constructs analyzed in Figure 3. Scale bars: 20μm (top), 5μm (bottom). (**B**) Wider view of DOR(MOR-ICL3)+linker or DOR(MOR-Ctail)+linker expressing cells to indicate proper plasma membrane expression of mutant receptors analyzed. Scale bars: 20μm (top), 5μm (bottom). (**C**) Representative confocal images of IMCD3 cells transiently expressing the indicated DOR constructs and labeled as described in **Figure 3**. Scale bars: 5μm. (**D**) Cilia enrichment analysis of DOR, DOR+linker, DOR(MOR-ICL3)+linker, and DOR(MOR-Ctail)+linker indicates that the MOR C-tail significantly enhances DOR cilia enrichment compared to DOR. One-way ANOVA (****$p<0.0001$) with Dunnett's multiple comparisons, data are represented as mean ± SEM from 3 independent experiments, 32-47 cells, (****) $p<0.0001$. Scale bars, 5μm. (**E**). Schematic of DOR+MOR constructs containing all of the DOR C-tail with progressive additions of the MOR C-tail. (**F**) Wider view of IMCD3 cells transiently transfected with DOR+MOR sufficiency as described in **Figure 3** demonstrating plasma membrane localization of all constructs. Arrows indicate cilia-localized receptor. Scale bars: 20μm (top), 5μm (bottom).

Figure S4.

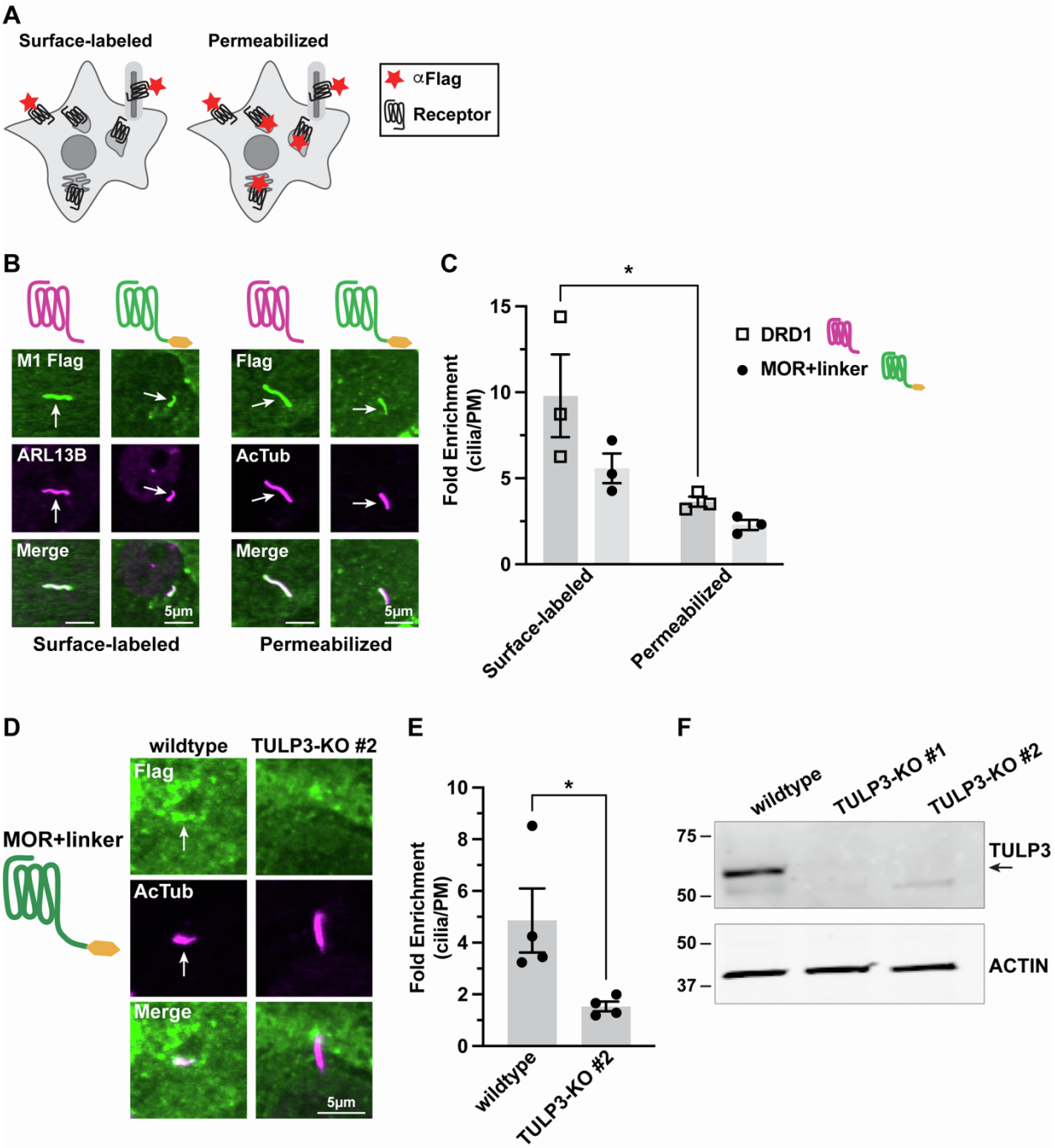

Figure S4. Comparison of staining techniques used in IMCD3 cells and additional TULP3-KO cell experiments supports a role of TULP3 in MOR cilia delivery. (**A**) Schematic of different receptor and cilia staining methods: Left: surface-expressed receptors are labeled prior to permeabilization in order to detect only the receptors trafficked to the cilium and cell surface. Right: all receptors are detected using the permeabilization method, thereby decreasing the relative ciliary receptor fluorescence compared to the whole cell. (**B**) Representative images of IMCD3 cells transiently expression DRD1 or MOR+linker. Cells were surface labeled with anti-Flag and cilia were

stained with anti-ARL13B (surface-labeled), or permeabilized and stained with anti-Flag and anti-AcTub (permeabilized). Scale bars: 5μm. (**C**) Image analysis demonstrates the reduction of ciliary fold enrichment with the permeabilization method (compare **Figure 2** (surface-labeled) to **Figure 4** (permeabilized). Two-way ANOVA interaction (ns) p=0.3; main effect of receptor (ns) p=0.0638; main effect of staining method (**) p=0.0065. Sidak's multiple comparison's test, data are represented as mean ± SEM from 3 independent experiments, 24-60 cells, (*) p=0.0198. (**D**) Representative images of wildtype (left) and TULP3-KO #2[1] (right) IMCD3 cells transiently transfected with MOR+linker. Cells were fixed and stained with anti-Flag and anti-AcTub antibodies. Scale bars: 5μm. (**E**) MOR+linker cilia enrichment was significantly reduced in TULP3-KO #2 IMCD3 cells than in wildtype. Student's t test, (*) p<0.038, data are represented as mean ± SEM, n=4 experiments, 77-79 cells. Scale bars, 5μm. (**F**) Western blot validation of TULP3 CRISPR/Cas9 knockout IMCD3 cell lines #1 (main text, **Figure 4**) and #2. Equal protein was loaded into wells and blot was probed for TULP3 and loading control ACTIN. Arrow indicates TULP3 protein band. Arrows indicate cilia-localized receptor.

Supplemental References

1. Ye, F., Nager, A.R., and Nachury, M.V. (2018). BBSome trains remove activated GPCRs from cilia by enabling passage through the transition zone. J Cell Biol *217*, 1847-1868. 10.1083/jcb.201709041.